

Crystallinity in poly(vinyl alcohol).

1. An X-ray diffraction study of atactic PVOH

Hazel E. Assender†* and Alan H. Windle

Department of Materials Science and Metallurgy, University of Cambridge,
 Pembroke Street, Cambridge CB2 3QZ, UK

(Received 7 October 1997; accepted 5 November 1997)

The significant level of crystallinity in atactic poly(vinyl alcohol) results from the comparatively modest size of the OH group enabling it to assume *d* and *l* positions in an atactic chain within a single crystal lattice. The structure is highly hydrogen bonded. An X-ray diffraction investigation has been made of the crystal structure to determine the distribution of hydrogen bonds, to understand the crystalline thermal expansion and to determine the influence of water on the polymer crystals and crystallisation process. Thermal annealing treatments have been developed to obtain samples of the maximum level of crystallinity with minimum disorder. The well-resolved diffraction peaks from such samples are analysed to measure the thermal expansion coefficients of the crystal unit cell which are related to the hydrogen bonding network in the crystal structure. Finally, the effect on the crystals of absorbing water into polymer of various levels of crystallinity and also during the crystallisation process is investigated, leading to the hypothesis that water molecules may be incorporated within the random crystal structure resulting in a change in the relative intensities of the diffraction peaks. © 1998 Elsevier Science Ltd. All rights reserved.

(Keywords: poly(vinyl alcohol); hydrogen bonding; crystallinity)

INTRODUCTION

Commercially produced poly(vinyl alcohol) (PVOH) is approximately atactic. It is made from the hydrolysis of polyvinyl acetate, and is found to contain 53% syndiotactic diads. N.m.r. evidence¹ indicates that the tacticity is random. In 1948, Bunn² suggested a crystal structure for PVOH that contained a random distribution syndiotactic and isotactic units. The well-known structure, shown in *Figure 1*, has two polymer molecules running through each unit cell. Each repeating monomer contains two hydroxyl sites, each with 50% occupancy, thus creating an atactic structure. The cell is monoclinic ($a = 7.81 \text{ \AA}$, $b = 2.52 \text{ \AA}$, $c = 5.51 \text{ \AA}$, $a = \gamma = 90^\circ$, $\beta = 91.7^\circ$) and thus, conforming to crystallographic convention, the polymer chains are described as lying along the *b*-axis of the unit cell. Bunn suggested two intermolecular hydrogen bonding directions, although recent molecular modelling results described in the second part of this series³ show that in addition to the intermolecular bonding, intramolecular hydrogen bonding is likely. The Bunn model for the crystal structure of PVOH has been shown to fit better than the structure proposed by Sakurada *et al.*⁴ (which also contains atactic chains) to both molecular modelling energy minimisations^{3,5} and experimental observations (for example Krimm *et al.*⁶). The Bunn and the Sakurada structures are shown in *Figure 2* for comparison. The difference between the two structures lies in the orientation of the molecules and the resulting intermolecular hydrogen-bonding directions within a very similar lattice.

Atactic PVOH has a high melting point ($T_m = 230^\circ\text{C}$) in comparison with polyethylene ($T_m = 117\text{--}135^\circ\text{C}$) as a result

of the high level of hydrogen bonding in the crystals (there are hydrogen bonding opportunities every second carbon atom). It is this hydrogen bonding which also controls the water solubility of the polymer, for although the amorphous regions of the polymer may be swollen by the ingress of water, the polymer will not dissolve until the crystal structure is broken down. Dissolution must involve the replacement of polymer–polymer hydrogen bonds with polymer–water hydrogen bonds.

PVOH is a material with technological potential as a water-processable polymer which would nevertheless be stable to the presence of water in everyday use. Control of solubility is currently achieved in a limited way by poorly understood heat and chemical treatments, and consequently the interaction of PVOH with water is the subject of considerable scientific and technological interest.

This paper seeks to understand better the crystallinity in PVOH by examination of the X-ray diffraction behaviour as a function of temperature and of annealing conditions. The interaction of water with the crystals is investigated, limited by the need to simultaneously control annealing and temperature. The relative peak intensities in the diffraction trace are shown later³ to be sensitive to the hydrogen bonding directions in the crystal, while the peak positions are sensitive to the intermolecular bonding which draws the molecules together.

SAMPLE PREPARATION

The polymer used in these experiments is Elvanol®, supplied by DuPont. The samples are atactic, and between 99.0% and 99.8% hydrolysed from poly(vinyl acetate). For examination by wide-angle X-ray powder diffraction, polycrystalline films of the polymer were cast from a 10 wt.% aqueous solution. The polymer was completely

* To whom correspondence should be addressed

† Present address: Department of Materials, University of Oxford, Parks Road, Oxford OX1 3PH, UK.

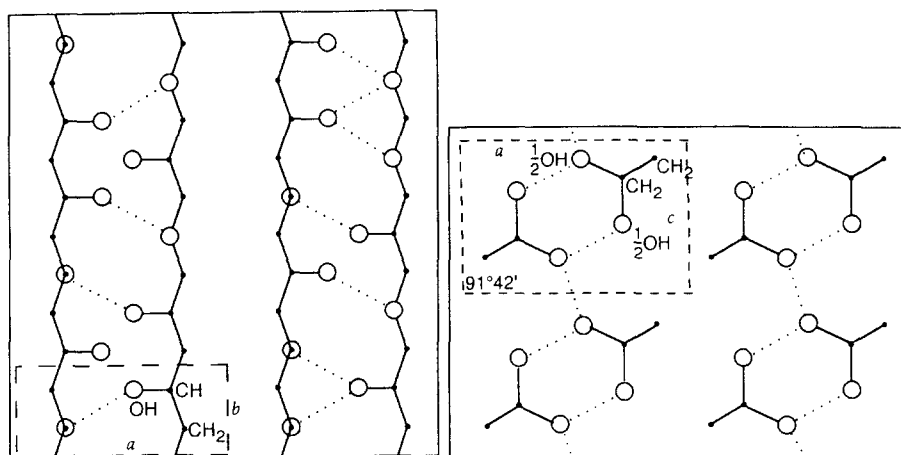


Figure 1 The crystal structure of PVOH as proposed by Bunn². Each unit cell contains two atactic chains. The -OH sites have 50% occupancy. The directions of intermolecular hydrogen as proposed by Bunn are shown by dashed lines

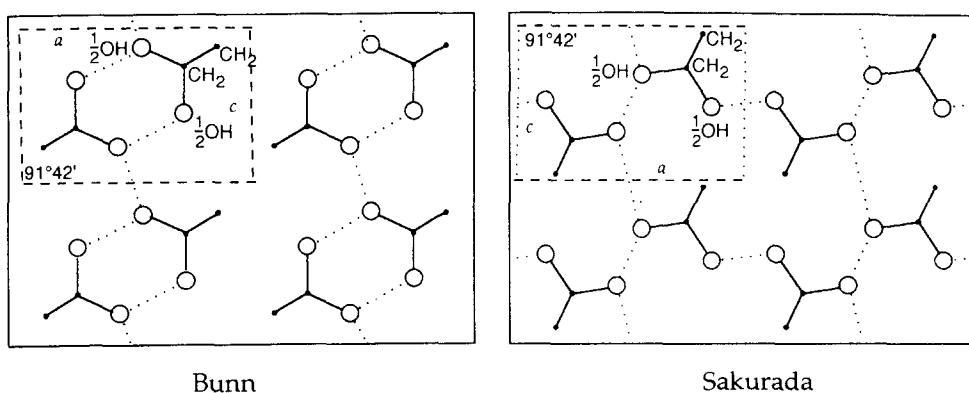


Figure 2 A comparison of the crystal structures of atactic PVOH as proposed by Bunn and by Sakurada. The two structures represent different models proposed from similar diffraction data and thus have the same unit cell parameters with appropriate transformations of the axes

dissolved in water at between 80 and 90°C with 30 min continuous stirring and cast onto glass, from which films 10–30 μm in thickness could be peeled. The water was removed from the solution, and the films completely dried by holding them at 50°C overnight. Once the films were cast, they were held in an atmosphere dried by silica gel. Films cast in this fashion were found to be around 30% crystalline, as measured by X-ray diffraction.

EFFECT OF ANNEALING TEMPERATURE ON CRYSTALS

A range of films prepared from aqueous solution and dried overnight at 50°C were annealed at different temperatures in the range 120–230°C in order to enhance the crystallinity, the samples being held between hot, thin PTFE sheets pressed onto a hot-plate. In each case the samples were annealed for periods which maximise the crystallinity at that temperature. For the lower temperatures this was about 1 h, and at the maximum temperature, 4 min. There was slight browning of those samples annealed at very high temperatures. After annealing, the samples were cooled rapidly on an aluminium block. The samples were turned over half-way through the annealing time. The development of crystallinity as a function of annealing temperature was then followed by recording X-ray powder diffraction traces from each sample after the annealing treatment. The series of diffraction traces is given in Figure 3, displaced from one

another by an amount proportional to the difference in temperature.

Crystallinities were determined from the traces in Figure 3; the areas under the crystalline and amorphous components of each trace being measured after the application of a standard Gaussian curve-fitting routine to the peaks. The degree of crystallinity is found to increase in the range 38–50% with increasing anneal temperatures from 120 to 230°C. These data should be compared with

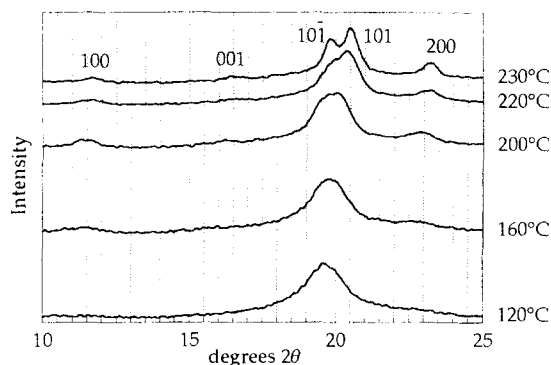


Figure 3 X-ray powder diffraction traces from films annealed at the temperatures indicated, showing the principal crystal diffraction peaks. The profiles are displaced from one another vertically by an amount proportional to the annealing temperature

studies made in which the crystallinity was determined by density measurements⁷. Samples produced both from direct hydrolysis of poly(vinyl acetate) films, and those cast from aqueous solution of pre-hydrolysed material, demonstrated increases in crystallinity in the range 41%–75%, with increases in annealing temperature in the range 90–210°C. On the other hand, measurements⁸ on PVOH crystals formed isothermally in the temperature range 100–170°C from a solution of triethylene glycol recorded a density of 1.301 g cm⁻³, irrespective of the crystallisation temperature, corresponding to 43 atm.% crystallinity in all cases, assuming a constant crystalline density of 1.345 g cm⁻³ and amorphous density of 1.269 g cm⁻³.

From our results, the crystal peaks are seen to shift to a higher Bragg angle corresponding to a decrease in unit cell dimension as the annealing temperature increases. The dimensional change is of the same order along both the *a*- and *c*-axes (perpendicular to the molecular axis). This improved packing within the crystals is interpreted as an improvement in crystal perfection which is also reflected in the increasing sharpness of the pattern. For the more highly crystalline samples prepared by annealing at the higher temperatures, the main diffraction intensity at around 20° 2θ resolves into a 10 $\bar{1}$,101 doublet. The doublet has been clearly resolved before in an X-ray diffraction measurement of a single crystal of atactic PVOH grown from 0.04% triethylene glycol solution by cooling from 200°C⁸.

THERMAL EXPANSION

Experimental

Thermal expansion coefficients of the crystal axes were carefully measured in the temperature range 20–210°C. In revealing the anisotropy of expansion, any structural transitions with temperature, and any variation in the unit cell shape or symmetry with temperature, the measurements give insight into the intermolecular bonding interactions within the crystal, in this case particularly the hydrogen bonding.

The thermal expansion of crystals in atactic PVOH was measured in 1964 by Ishikawa and Miyasaka⁹ from X-ray diffraction photographs taken from highly drawn and heat-treated fibre samples. The measurements successfully demonstrated a distinct change in the linear thermal expansion coefficients along all three axes at a crystal transition observed at around 120°C. This transition had been previously observed as a discontinuous change in specific volume¹⁰, dynamic properties¹¹ and relative intensity of the crystallinity sensitive infra-red absorption band¹², and had been indefinitely attributed to the crystallites. The thermal expansion measurements could not resolve the 10 $\bar{1}$ and 101 diffraction intensities centred at about 19.4 and 20.0° 2θ, respectively, and so any variation with temperature in the monoclinic angle could not be measured, and the angle was assumed to remain constant during the expansion.

By producing highly crystalline samples through careful annealing treatment, we have been able to resolve the 10 $\bar{1}$ and 101 peaks in the powder X-ray diffraction traces, and thus monitor any change in the monoclinic angle. X-ray powder diffraction measurements over the range 15–25° 2θ were made on a series of highly crystalline samples (previously annealed for 5 min at 230°C and quenched) each sample being held isothermally in the range 20–210°C during the diffraction measurement. The maximum

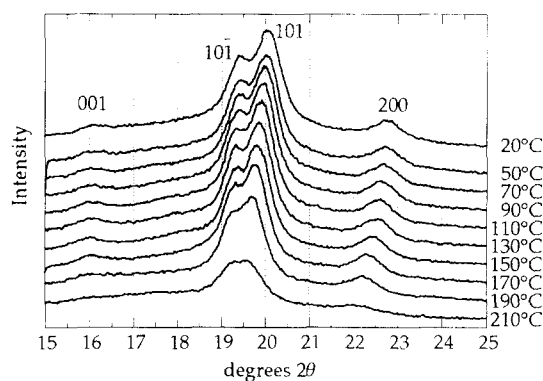


Figure 4 A series of powder diffraction traces in the angular range 15–25° 2θ taken at various of temperatures in the range 20–210°C. The traces have been vertically displaced from one another by an amount proportional to the measurement temperature. The observed changes are all recoverable with temperature

measurement temperature was 210°C, the greatest temperature at which the sample could be held without observable permanent change to the room-temperature diffraction profile as a result of the heat treatment during the scan. Within the recorded temperature range, any change in the diffraction behaviour at temperature was fully reversible on cooling. *Figure 4* shows the diffraction traces as recorded for each of the different temperatures, displaced from one another vertically, for clarity, by an amount proportional to the sample temperature. The whole series of scans was repeated using a separately prepared sample, and showed excellent agreement. Within this angular range there are four crystalline maxima which may be indexed as 001 at 2θ ≈ 16.1°, 10 $\bar{1}$ at 2θ ≈ 19.4°, 101 at 2θ ≈ 20.0° and 200 at 2θ ≈ 22.7° (angles are those at 20°C). Each of these curves was fitted to a function made up of the sum of five Gaussian functions (one for the amorphous halo, and four corresponding to the crystal intensities) and the peaks of the crystalline maxima of the fitted function recorded. From these four crystal peaks, the unit cell lengths *a* and *c*, and the monoclinic angle β may be calculated*. Each of these parameters is plotted as a function of temperature in *Figure 5*. The data from both sets of experiments are included. It is possible to fit two linear regions above and below a transition at around 130°C. The fit is drawn in the final (percentage change) plot in *Figure 5*. The thermal expansion coefficients for each parameter above and below the transition are tabulated in *Table 1* alongside those determined assuming no change in β by Ishikawa and Miyasaka⁹ who did not have the benefit of 10 $\bar{1}$ /101 resolution. The powder diffraction measurements do not show a strong, well-resolved peak including a *b*-axis component, and so no measurement of the thermal expansion coefficient along the chain axis was made from these data.

Both sets of data showed a considerably greater thermal expansion of the unit cell along the *a*-axis than along *c*, both above and below the transition temperature. This result is consistent with the Bunn model for the crystal structure (but not that of Sakurada), where along the *c* direction there is a continuous chain of covalent and hydrogen bonding making the crystal less able to expand in response to temperature

* *a*, *c* and β as quoted here were calculated from the three strongest intensities 10 $\bar{1}$, 101 and 200, although a cross check with the 001 peak proved to be in good agreement.

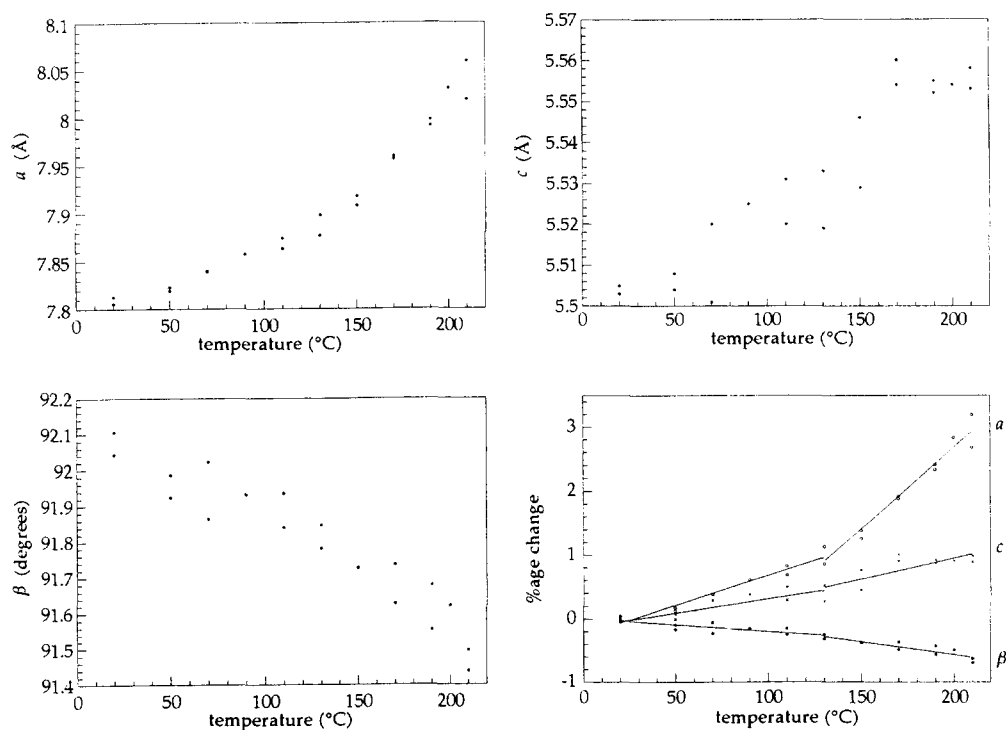


Figure 5 The unit cell parameters a , c and β , and the percentage change in the three parameters plotted as a function of temperature, with linear curve fits to the percentage change data of the thermal expansion coefficient above and below a crystal transition at about 130°C

Table 1 Linear thermal expansion coefficients for the unit cell parameters a , c and β as calculated from the linear fits in *Figure 5*, and those measured by Ishikawa and Miyasaka⁹

	Assender and Windle		Ishikawa and Miyasaka	
	Below 130°C	Above 130°C	Below 130°C	Above 130°C
$\alpha_a (\times 10^{-4})$	0.93 ± 0.07	2.46 ± 0.18	1.1 ± 0.1	2.4 ± 0.1
$\alpha_c (\times 10^{-4})$	0.44 ± 0.09	0.67 ± 0.16	0.3 ± 0.05	1.0 ± 0.2
$\alpha_\beta (\times 10^{-4})$	—	—	0.0 ± 0.01	-0.15 ± 0.05
$d\beta/dT (\times 10^{-3})$ (β in degrees)	-2.0 ± 0.4	-3.8 ± 0.6	—	—

than along the a -axis where there is no such continuous chain. The overall increase in the magnitude of the thermal expansion coefficients above the transition at 130°C indicates a weakening in interchain bonding.

The kink model

An increase in the thermal expansion coefficients above a particular temperature is a characteristic of several other polymer systems such as PE¹³ and polyoxymethylene¹⁴ and is usually associated with some increase in the freedom of chains to undergo conformational rotation. One point of view is that the distinct change in expansion coefficients corresponds to the generation of kink-type defects in the chain. The generation of kinks has been discussed in detail for the case of the thermal expansion of polyethylene above 65°C ¹³. In the case of PVOH, the observation of the zero coefficient of expansion of the b (chain) axis below 130°C and a contraction above this temperature (Ref. 9 and *Table 1*) has recently been accounted for by Nakamae *et al.*¹⁵ in terms of the onset of the formation of backbone kink defects at 130°C . There are, however, a number of difficulties associated with such an interpretation:

(a) It is not apparent that the introduction of kinks such as that shown in *Figure 6a* in a crystal would generate the changes in lattice parameters parallel and

perpendicular to the molecular axis that are shown by X-ray diffraction.

(b) There is a reduction in elastic modulus along the chain axis corresponding to the 'transition', and Nakamae *et al.*¹⁵

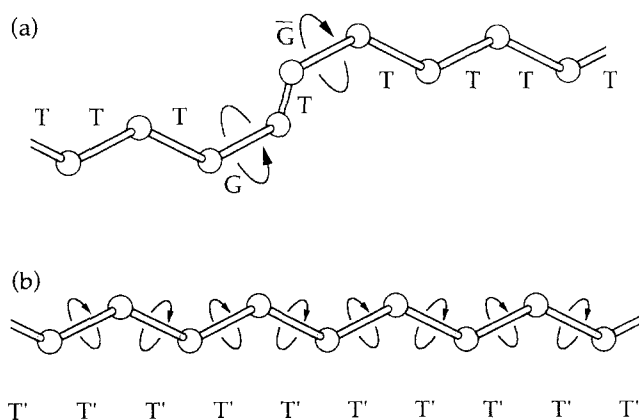


Figure 6 Schematic representations of a polymer molecule after thermal contraction illustrating (a) the kinked chain model and (b) the homogeneous internal rotation model proposed by Nakamae *et al.* (reproduced from Ref. 15)

suggest that such an effect could not be accounted for in terms of a homogeneous change in backbone torsional angles as shown in *Figure 6b*. However, their modulus calculations were made considering only an isolated chain of polymer which give values much smaller than are predicted when a chain with similar defects is modelled within a crystal lattice¹⁶.

(c) The kink model, as developed, provides no explanation for the observed anisotropy in the increased lateral expansion above 130°C.

Overall, it appears that the kink model is introduced to provide a rationale for the change in expansion coefficients at 130°C, while there appears to be very little direct evidence which supports it. It should also be pointed out that our calculations indicate that homogeneous variations in torsion angles of no more than $\pm 4^\circ$ (organised in the regime $+\phi$, $+\phi$, $-\phi$, $-\phi$ to preserve chain linearity) are sufficient to account for the reported (negative) thermal expansion coefficient along the chain axis in the temperature range 20–200°C.

Breaking of hydrogen bonds with increasing temperature

If the kink model is to be discounted, there is still the necessity to explain the increased mobility of the molecules in the crystals above 130°C. In some way, the influence of either intramolecular or intermolecular bonding (or both) decreases at the transition. In nylon systems at high temperatures, the polymer undergoes a Brill transition in which the amide unit is able to rotate by 60° to create a new hydrogen bonding direction¹⁷. This transition is reflected in the changes to the X-ray diffraction pattern which indicate a transition from monoclinic to pseudo-hexagonal for the case of nylon 8 above about 160°C, for example. The transition is also associated with a 3% reduction in the repeat length along the molecular axis¹⁸.

We turn back to PVOH now and the hydrogen bonding regime of the general form due to Bunn. We include intramolecular hydrogen bonding in the crystal as discussed

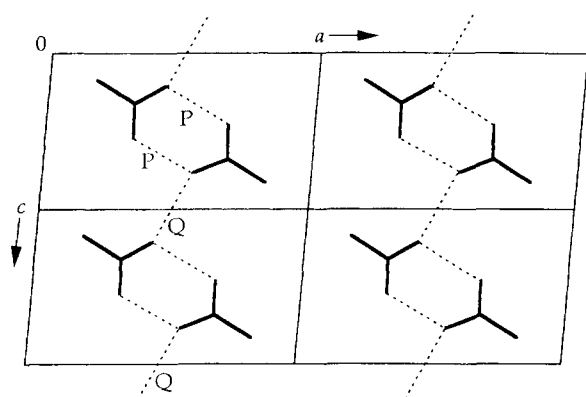


Figure 7 Schematic of the Bunn crystal structure of PVOH projected onto the (010) plane (i.e. viewed along the molecular axes) showing the two intermolecular hydrogen bonding directions (dashed lines) labelled P and Q

Table 2 Linear thermal expansion coefficients of the crystal unit cell along the [101] and $[\bar{1}02]$ directions as calculated from the data in *Figure 4*

	Below 130°C	Above 130°C
$\alpha_{[101]} (10^{-4})$	0.94 ± 0.16	2.20 ± 0.42
$\alpha_{[\bar{1}02]} (10^{-4})$	0.44 ± 0.25	0.98 ± 0.08

in the second paper of this series. One possibility is that the intramolecular hydrogen bonds begin to break down providing the additional conformational mobility of the chains indicated by the onset of the transition. It is worth noting that Ishikawa and Miyasaka⁹ found no change at all in the chain axis repeat length below 130°C, an indication perhaps of intramolecular hydrogen bonding impeding a reduction in the molecular repeat length. The lateral coefficient of the thermal expansion increases by a factor of 2.5 at the same temperature, which suggests that the interchain hydrogen bonds might similarly be involved.

As illustrated in *Figure 7*, there are two types of interchain hydrogen bonding, type P aligning approximately with [1V1] and type Q approximately with $[\bar{1}V2]$. (The use of the general index 'V' in the indices rather than '0' implies that the interchain hydrogen bonds are not necessarily normal to the chain axis).

Firstly, it should be noted that the comparatively rapid expansion along the *a*-axis above the transition is not accompanied by any significant change in the relative intensities of the diffraction peaks (see *Figure 4*). The implication is that the chains move pro rata with the expansion in *a*, implying that the P bonds holding the chains in pairs are no longer especially influential. It follows, therefore, that the anisotropy of expansion ($\alpha_a > \alpha_c$) would require the P bonds breaking more than the Q-type, a point illustrated by the resolution of the lateral thermal expansion coefficients onto the projections of the two bond directions onto the plane perpendicular to the chain axis, as tabulated in *Table 2*. Any independent twisting of the molecular backbones would result in a lengthening of the P-type bonds, whereas the Q bonds are much more able to adjust their direction without resulting in a change to the hydrogen bond length to accommodate the backbone distortion. The suggested process of thermal expansion is shown schematically in *Figure 8*.

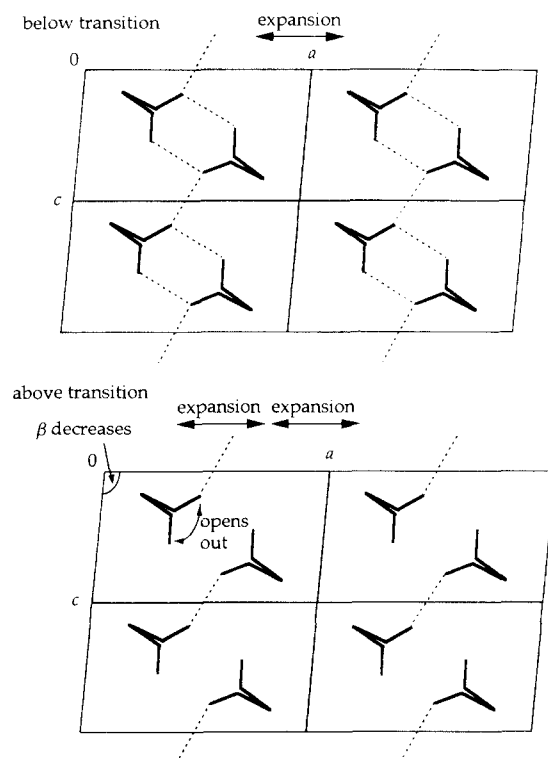


Figure 8 Schematic illustrating the thermal expansion of the crystal structure above and below the transition at 130°C

Furthermore, the simulation of X-ray scattering from PVOH crystals described in Part II of this series has demonstrated, somewhat surprisingly, that the relative intensities of the peaks are sensitive to the directions of the OH bonds, so that although it appears some hydrogen bonds are broken with increasing temperature, the average directions of the OH bonds are not markedly changed.

POLY(VINYL ALCOHOL) CRYSTALS AND WATER

Water in the amorphous phase

The glass transition temperature of the polymer is reduced by the ingress of water into the amorphous regions, the water acting as a plasticiser. The glass transition was measured in a series of unannealed PVOH films equilibrated in a range of relative humidities by dielectric thermal analysis. The temperature of the α relaxation, associated with the glass transition temperature, was defined as the maximum in the dielectric loss on application of an alternating electric field. The α relaxation was measured at a series of frequencies; the results are given in *Figure 9*. The samples were each cast from aqueous solution, dried at 50°C and then equilibrated overnight in an atmosphere of the desired relative humidity in a sealed container. The films were removed from the humidity chambers before analysis and clamped between two flat metal plates for testing. The samples were tested as rapidly as possible to minimise water transfer with the minimum surface area exposed, but inevitably as the sample temperature increased, water would be removed. The loss of water during the test became increasingly significant above 100°C, and accounts for the fact that the change in T_g with initial water content was barely detectable at 10 Hz (T_g around 190°C). Note that at the lowest frequency measurement, the T_g lies below ambient temperature in the samples equilibrated in high humidity.

The amorphous component of the PVOH is shown to be influenced by the absorption of water, but in order to examine whether water affects the crystalline phase, a series of comparisons between samples given various heat and humidity treatments was undertaken, and the resulting X-ray powder diffraction traces compared.

The influence of water on the crystalline phase

A comparison between a sample cast from aqueous solution and dried and one cast, dried, exposed to 97% relative humidity overnight and redried produces a pair of

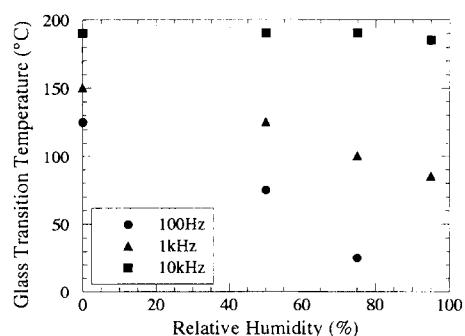


Figure 9 The glass transition temperature of a series of PVOH films kept under various relative humidities measured by dielectric thermal analysis (DETA) at three decades of frequency. The glass transition temperature decreases with increasing humidity which corresponds to increasing amounts of water in the amorphous regions of the polymer

identical diffraction patterns, as one would expect. Similarly, samples annealed for 5 min at 230°C to produce a maximum level of crystallinity showed no change in the powder diffraction trace on subsequent humidity treatment, suggesting that crystals formed by this annealing process do not absorb water.

The presence of water *during* the crystallisation process, however, does influence the resulting diffraction trace. A comparison was made between a sample crystallised by annealing at 100°C for 10 min under dry conditions and a second sample which was equilibrated to 97% relative humidity, and then annealed under water vapour at 100°C before drying. *Figure 10* shows the two resulting traces. The sample annealed in humid conditions shows a significantly higher degree of crystallinity with the main peak shifted to slightly higher angles (shorter repeat distance). The enhanced crystallinity arises from the plasticising effect of the water. At 100°C, the polymer is only just above its dry T_g (as measured, for example, by d.s.c.), but under wet conditions the polymer is far above its glass transition facilitating crystallisation. In summary, holding the polymer in high humidity does not break down any crystallinity formed in the sample during annealing treatments, but the water will serve to plasticise the polymer and enhance any crystal growth and perfection process if it is present during annealing.

To investigate any effect of the presence of water on the crystal structure (as has been suggested after n.m.r. studies^{19,20}), a highly crystalline sample must be produced which shows sharp, well-resolved, diffraction peaks. To this end, a series of samples were equilibrated under a range of relative humidities and annealed, from that condition, for 5 min at 230°C between PTFE sheets. As in the case of the DETA measurements, the water will be evaporating from the sample as the temperature is raised, but those samples equilibrated under higher humidities will have more water present during the crystallisation process. The series of diffraction traces from samples annealed from different relative humidities is shown in *Figure 11*. The data are plotted over a smaller angular range to highlight the predominant crystal peaks. As the relative humidity increases, the main diffraction peaks ($10\bar{1}$ and 101) become more resolved. In addition, as the humidity immediately before annealing increased the relative intensities of the $10\bar{1}$ and 101 peaks reversed. Samples crystallised dry have the higher angle peak (corresponding

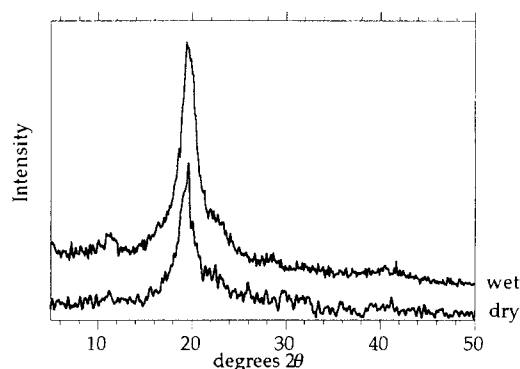


Figure 10 Powder X-ray diffraction traces of PVOH films annealed at 100°C for 10 min. The lower trace is from a sample dried with silica gel, and the upper trace, displaced for clarity, is from a sample equilibrated under 97% relative humidity, annealed under a humid atmosphere and dried before X-ray analysis

to the 101 lattice spacing) of greatest intensity, but as the concentration of water present during crystallisation increases, the lower angle, 10 $\bar{1}$ peak becomes dominant. No dry annealing treatments have yet been found to produce a pattern with 10 $\bar{1}$ as the most intense peak. The peak positions were analysed as described above to determine a , c , and β . The lattice dimensions decrease anisotropically with increased humidity (Figure 12), but the monoclinic angle changes only slightly as the water present during crystallisation increases. The scatter in the data does not allow analysis of the exact form of the relation between water concentration and peak positions.

A possible scheme to account for the change in the X-ray diffraction traces when water is present during crystallisation may be considered by a close examination of the crystal structure. In PVOH, where atactic sections of the polymer chain are incorporated into a crystal structure, each OH group can lie in one of two sites depending upon the polymer's local stereochemistry, each of these sites being, on average, 50% occupied. Consequently, there exists some free volume within the crystal corresponding to unoccupied sites. A water molecule is of comparable size to the OH group, and so it would, perhaps, not be surprising to conclude that water molecules could be incorporated into the PVOH crystal lattice if they were present during the crystallisation process. The oxygen atom of the water would not, however, be able to sit precisely in the vacant site of a polymer OH group as it is not covalently bonded to the carbon backbone. The crystal structure of atactic PVOH has

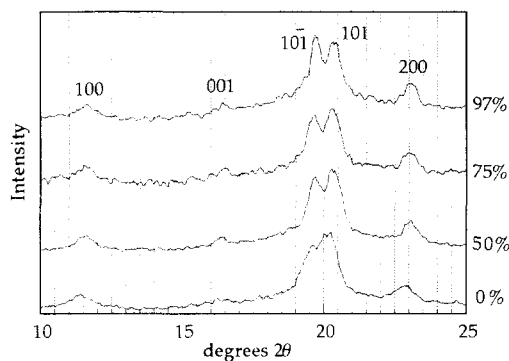


Figure 11 A series of room temperature X-ray diffraction traces from samples annealed for 5 min at 230°C. Immediately prior to annealing, each sample had been equilibrated under a different relative humidity from 0% (under silica gel) to 97%. The traces are displaced vertically from one another for clarity

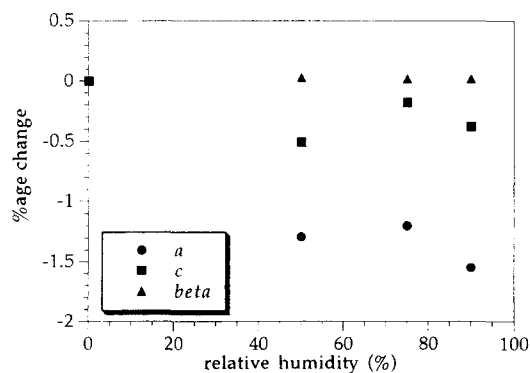


Figure 12 The percentage change in unit cell dimensions from a those of a sample annealed dry, for samples annealed from various water contents. The data are taken from the diffraction traces shown in Figure 11

been modelled by the authors in part two of this series³ using a molecular mechanics approach, and a further account of the structural implications of water in the crystals is given there.

CONCLUSIONS

Increasing the annealing temperature in the range 120–230°C is found to increase the maximum level of crystallinity achievable from 38 to 50 atm%. As the annealing temperature increases, the diffraction peaks became sharper as a result of increased structural perfection in the crystals. Annealing at 230°C for 5 min allowed the 10 $\bar{1}$ and 101 diffraction peaks to be resolved.

The thermal expansion coefficient of the crystal changes at around 130°C, and the monoclinic angle decreases with increasing temperature, also showing a transition at 130°C. The thermal expansion is more marked along the a axis of the unit cell, as expected from the Bunn model of the crystal structure.

The change in thermal expansion coefficients at 130°C is explained in terms of a break-down in the hydrogen bonding network in the crystal resulting in an increased mobility for the polymer chains to twist away from a planar zig-zag conformation. The 'kinked chain' model of thermal expansion does not fit the expansion data measured.

The glass transition temperature of the polymer is decreased with increasing water concentration in the polymer. This enhances the crystallisation process when water is present resulting in a greater level of crystallinity on annealing. Once crystals are formed in the dry, their diffraction profile appears to be unaffected by water absorbed into the polymer, but crystals formed in the presence of water show a reversal in the relative intensities of the 10 $\bar{1}$ and 101 peaks.

ACKNOWLEDGEMENTS

The authors wish to thank DuPont for provision of samples, Dr A.J. East of Hoechst Celanese Corporation, New Jersey, and Dr S. Moratti of the Melville Laboratory for Polymer Synthesis, Cambridge, for their contributions, and the EPSRC for funding.

REFERENCES

- Horii, F., Hu, S., Ito, T., Odani, H., Kitamaru, R., Matsuzawa, S. and Yamaura, K., *Polymer*, 1992, **33**, 2299.
- Bunn, C.W., *Nature*, 1948, **161**, 929.
- Assender, H. E. and Windle, A. H., *Polymer*, 1998, **39**, 4303.
- Sakurada, I., Fuchino, K. and Okada, N., *Bull. Inst. Chem. Res., Kyoto Univ.*, 1950, **23**, 78.
- Kusanagi, H. and Ishimoto, A., in *Computer Aided Innovation of New Materials II*, ed. M. Doyama, J. Kihara, M. Tanaka, and R. Yamamoto. Elsevier Science, 1993, p. 1365.
- Krimm, S., Liang, C.Y. and Sutherland, G.B.B.M., *J. Polym. Sci.*, 1956, **22**, 227.
- Kenney, J.F. and Holland, V.F., *J. Polym. Sci. Pt A-1*, 1966, **4**, 699.
- Kenney, J.F. and Willcockson, G.W., *J. Polym. Sci. Pt A-1*, 1966, **4**, 679.
- Ishikawa, K. and Miyasaka, K., *Reports Prog. Polym. Phys. Japan*, 1964, **7**, 93.
- Yano, Y., *Busseiron Kenkyu*, 1956, **94**, 176.
- Takayanagi, M. *et al.*, *The Third Symposium on PVA*, Japan, 1963.
- Nagai, E., *Polyvinyl Alcohol*, 1955, p. 245.
- Nishino, T., Ohkubo, H. and Nakamae, K., *J. Macromol. Sci.-Phys. B*, 1992, **31**, 191.
- Nakamae, K., Nishino, T., Shimizu, Y. and Hata, K., *Polymer*, 1990, **31**, 1909.

15. Nakamae, K., Nishino, T., Ohkubo, H., Matsuzawa, S. and Yamaura, K., *Polymer*, 1992, **33**, 2583.
16. Renker, D.H. and Mazur, J., *Polymer*, 1984, **25**, 1549.
17. Atkins, E.D.T., Hill, M.J. and Veluraja, K., *Polymer*, 1995, **36**, 35.
18. Vogelsong, D.C., *J. Polym. Sci. A*, 1963, **1**, 1055.
19. Gupta, R.P., *J. Polym. Sci. A*, 1965, **3**, 3951.
20. Terao, T., Maeda, S. and Saika, A., *Macromolecules*, 1983, **16**, 1535.